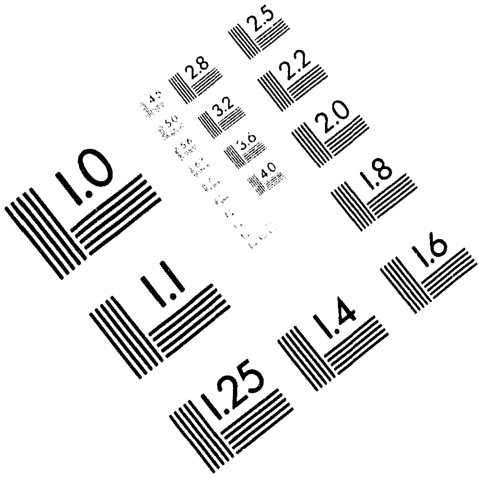

AIIM

Association for Information and Image Management

1100 Wayne Avenue, Suite 1100
Silver Spring, Maryland 20910

301/587-8202

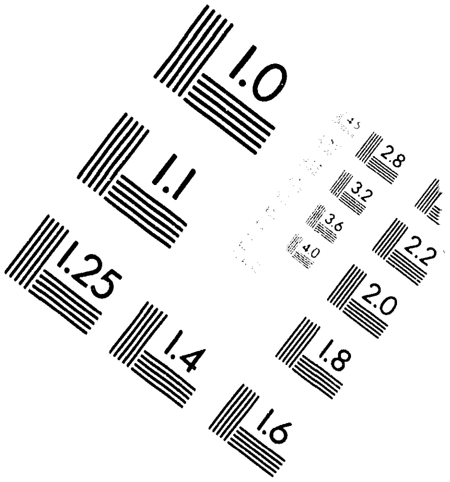

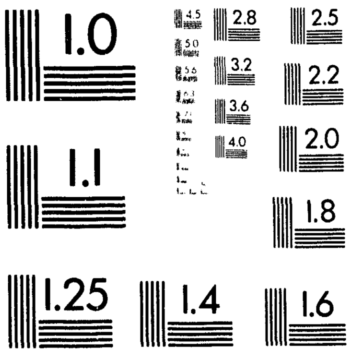

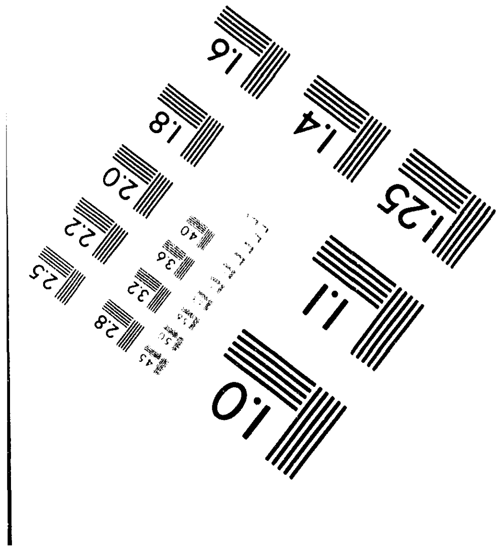

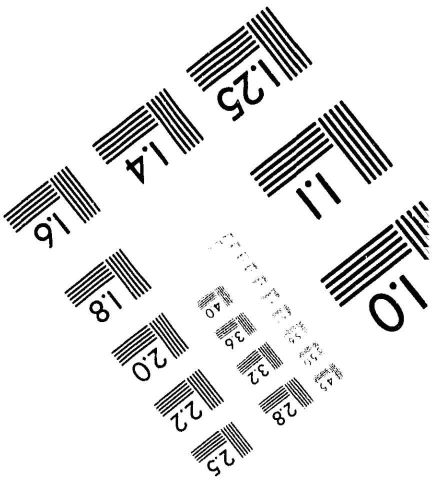

MANUFACTURED TO AIIM STANDARDS
BY APPLIED IMAGE, INC.

1 of 1

UCRL-ID-116779

Progress Report of Foam Shell Project

G.E. Overturf
D. Schroen-Carey
B. Reibold
R.C. Cook

March 25, 1994

Lawrence Livermore National Laboratory

Work performed under the auspices of the U.S. Department of Energy by the Lawrence Livermore National Laboratory under Contract W-7405-Eng-48.

DISCLAIMER

This document was prepared as an account of work sponsored by an agency of the United States Government. Neither the United States Government nor the University of California nor any of their employees, makes any warranty, express or implied, or assumes any legal liability or responsibility for the accuracy, completeness, or usefulness of any information, apparatus, product, or process disclosed, or represents that its use would not infringe privately owned rights. Reference herein to any specific commercial products, process, or service by trade name, trademark, manufacturer, or otherwise, does not necessarily constitute or imply its endorsement, recommendation, or favoring by the United States Government or the University of California. The views and opinions of authors expressed herein do not necessarily state or reflect those of the United States Government or the University of California, and shall not be used for advertising or product endorsement purposes.

This report has been reproduced
directly from the best available copy.

Available to DOE and DOE contractors from the
Office of Scientific and Technical Information
P.O. Box 62, Oak Ridge, TN 37831
Prices available from (615)576-8401, FTS 626-8401

Available to the public from the
National Technical Information Service
U.S. Department of Commerce
5285 Port Royal Rd.,
Springfield, VA 22161

Date: March 1, 1994 TST 94-033

To: Distribution

From: George Overturf, Bob Reibold, and Bob Cook, LLNL
Diana Schroen-Carey, WJSA

Subject: Progress Report of Foam Shell Project

Summary:

We report on our work to produce a foam shell target for two possible applications: 1) as liquid-layered cryogenic target on Omega Upgrade, and 2) as a back-up design for the NIF. This target consists of a roughly 1 mm diameter and 100 µm thick spherical low-density foam shell surrounding a central void. The foam will be slightly overfilled with liquid D_2 or DT, the overfilled excess being symmetrically distributed on the inside of the shell and supported by thermal gradient techniques. The outside of the foam is overcoated with full density polymer which must be topologically smooth. The technology for manufacturing this style of foam shell involves microencapsulation techniques and has been developed by the Japanese at ILE. Our goal is to determine whether this technology can be successfully adapted to meet US ICF objectives. To this end a program of foam shell development has been initiated at LLNL in collaboration with both the General Atomics DOE Target Fabrication Contract Corporation and the Target Fabrication Group at LLE.

We have produced foam shells of the required diameter and wall thickness using the Japanese techniques. We have also constructed a microencapsulating droplet (water in oil in water) generator. We have found that the kinetics of the subsequent polymerization of the oil phase to form the foam depends intimately on solvent purity. Significant problems continue in the areas of foam wall thickness uniformity. We have developed techniques to streamline the various solvent exchange steps using Soxlet extraction devices. We are beginning to work with poly(vinyl phenol) as an overcoating polymer, following Japanese reports that smoother outer surfaces can be achieved. We have also prepared bulk foam samples for use in quantifying the problem of achieving optical access though the opaque foam wall adequate for monitoring the liquid-layering process.

Introduction and Background:

The long term objective of this project is to develop the technology for the production of overcoated foam shells that will be suitable for use as targets supporting a cryogenic liquid D_2 (or DT) fuel layer. The foam shell technology that is being explored was (and is still being) developed by the Japanese, the lead investigators being and T. Norimatsu M. Takagi at Osaka[1-6] and by H. Kim at LLE.[7,8] The initial use of these targets is planned for Omega Upgrade at LLE, however if the technology (both foam shell and subsequent liquid layering) is successful, this target design would provide an alternative to the solid cryogenic fuel layers currently planned for the NIF.

Our short term objective is to provide usable foam materials and shells in order to test the liquid layering technology being developed under the National Cryogenic Target Program. A key problem to overcome is the opaqueness of the foam shell which limits optical access. For cryogenic layering studies, we need to be able to determine liquid layer thicknesses to within about one micron. The current foam system has a cell size on the order of one micron and its index of refraction is 1.55. This poor match to the index of refraction of liquid deuterium (1.13) coupled with the large cell size causes considerable light scattering. Thus our current optical diagnostics may be insufficient. Our initial objective is to provide materials that will allow quantitative evaluation of the problem. If it is found that inadequate optical access is available, there are two alternatives: (1) modify the diagnostics, or (2) explore foam materials with smaller length scale microstructures.

By way of background, let us first review the steps in the shell formation process as developed by the Osaka group. Small droplets of water are microencapsulated by a 4 wt% solution of trimethylol propane trimethacrylate (a trifunctional polymerizable monomer) in dibutyl phthalate which has a density closely matched to the aqueous phase. These microencapsulated droplets are suspended in another aqueous phase and stabilized against coagulation by polyvinyl alcohol (PVA). Polymerization is thermally initiated resulting in the gelation and chemical crosslinking of the polymerizable monomer throughout the oil phase. These solvent impregnated foam shells are collected and the dibutyl phthalate and most of the interior water are replaced with toluene. A subsequent solvent exchange is made with ethanol to insure that all the water has been removed. The ethanol is then replaced with a *p*-chlorotoluene solution of isophthaloyl chloride, a diacid chloride. The foam shells filled with this solution are then introduced into an aqueous solution of hydroxyethyl cellulose (HEC), or more recently poly(vinyl phenol) (PVP). As the diacid chloride molecules diffuse out from the foam shell they react with and crosslink the HEC or PVP at the oil-water interface to form a full density layer surrounding the foam shell. The solvent in this overcoated shell is then exchanged for dioxane and the shells are placed in a Polaron pressure vessel. The dioxane is then exchanged for liquid CO_2, which is subsequently removed supercritically to preserve the structure of the low density foam shell.

Earlier (TST 93-246; 11/12/93) we outlined our progress in duplicating the Osaka method and some of the problems encountered. We had made enough batches of shells to have "seen" the process all the way through. The shells that we obtained were in general inferior to those Osaka has reported. Our results were initially inconsistent, due to a lack of complete understanding of the details of the various Osaka method steps, and due to the lack of a reliable method for producing the initial microencapsulated droplets. Some of these problems have been eliminated.

In what follows we document progress since our last report. Following the order presented in the above summary of the method, we have broken our presentation into sections focusing on droplet generation for the formation of the initial microencapsulated droplets, polymerization and gelation issues, solvent exchanges and improving their efficiency, and overcoating issues. In a final section we also report on the preparation and characterization of bulk samples for light scattering studies to determine the roadblocks to optical access in future liquid layering experiments.

Microencapsulated Droplet Generation

One immediate goal is to produce an inventory of foam shells with diameters of about 1 mm and wall thicknesses of about 100 µm. The shake and toss process of microencapsulation produces broad distributions of diameters and wall thicknesses, only some of which are of interest. Furthermore, the shake and toss process is prone to making homogeneous foam beads, as well as foam shells with internal foam beads. It is common to have both defects in the same shell batch. We believe these defects result from the uncontrolled mixing of the internal water phase and the organic phase. Too little mixing traps no water phase within the organic, and a foam bead is created. Too much mixing traps extra portions of organic phase within the internal water phase, and internal beads are made. These internal beads range in diameter from a few to hundreds of microns. To help eliminate these problems, and to give us control over both the microencapsulated droplet size and oil phase wall thickness, we have constructed a droplet generator.

In any generator of microencapsulated droplets one needs a multiple orifice system. We carefully examined the Osaka design and the design used at Soane Technologies, borrowing an operating version of the latter for testing. We were looking for an orifice system that would work simply and under a variety of flow rates to give us size and wall thickness control. We settled on a triple orifice system, similar to the Osaka design. A schematic of our system is shown in Figure 1. The inner orifice delivers the internal water phase. An orifice surrounding this delivers the oil phase that contains the polymerizable monomer. One difference between our design and Osaka's is that the length of our inner-most orifice is adjustable. We found that having the inner orifice either slightly inside or slightly beyond the second orifice was advantageous in stabilizing the water stream within the organic stream. This two phase stream must then be broken into droplets and delivered into the external water phase. The size of the microencapsulated droplet will depend on how this break-up is done. For a given microencapsulated droplet size, the relative flow rates of the inner water phase and surrounding oil phase will determine the oil phase wall thickness.

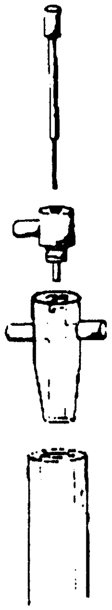

First Orifice - Dispenses the internal water phase, driven by a precision peristatic pump. The depth of this needle is adjustable even during operation of the system.

Second Orifice - Dispenses organic phase, driven by a syringe pump.

Third Orifice - Dispenses external water phase, from two ports, driven by a syringe pump. The rate determines the outer diameter of the shell produced. This orifice is clear plastic to allow observation of the microencapsulation process.

Tygon Tubing - Attaches to the bottom of the third orifice, approximately one meter in length. This allows us to study the preforms and select groups of preforms.

Figure 1. Shown is an exploded view of the LLNL droplet generator orifice construction.

For a microencapsulated droplet with diameter *d* and oil phase wall thickness *w* the volumes *V* of the inner aqueous water phase (V_w) and outer oil phase (V_o) are

$$V_w = \frac{4}{3}\pi\left(\frac{d}{2} - w\right)^3$$

and

$$V_o = \frac{4}{3}\pi\left(\frac{d}{2}\right)^3 - V_w$$

respectively. The ratio of the volume rates of flow of the oil phase to the water phases is simply the ratio of these volumes:

$$\dot{V}_o / \dot{V}_w = V_o / V_w$$

Thus for a 1.2 mm encapsulated droplet with an oil wall thickness of 100 µm we want the ratio of the oil to water flow rates to be about 0.7. The flow rates are controlled by a peristaltic pump for the internal water phase and a syringe pump for the oil phase. Since only the ratio of flow rates is relevant, we have set the internal water flow rate at 0.1 mL/h, which corresponds to the delivery of a 1 mm drop of water every 1.9 sec. With an oil phase flow rate of about 0.07 mL/h we will produce 100 µm thick walls if we break the stream into 1.2 mm droplets. The flow rate of the outer water phase is also controlled by a syringe pump and is adjusted to break off encapsulated droplets at a frequency appropriate for the desired size, about 1 every 1.9 sec in the example given. Unlike the Japanese system we are currently not using any sort of imposed frequency modulator to enhance droplet break-up since there is no apparent need. Thus, in summary, overall size is controlled by the outer stripping aqueous phase flow rate and wall thickness by the relative flow rate of the oil to water phases.

The outer orifice which supplies the stripping fluid is a Plexiglas sleeve, and is followed by a meter of tygon tubing through which the encapsulated droplets flow to the collection vessel. The transparency of the Plexiglas and tygon tubing allows us to easily monitor (and film for later examination) the droplet breakup frequency. It is very easy to see fluctuations in the system since they affect the otherwise even spacing between the microencapsulated droplets. We are also able to inspect the droplets in the tubing under low magnification to confirm that they have the correct diameter and wall thickness. The train of droplets in the tygon tubing is stable enough that it is possible to stop the flow of the carrier water phase and study the individual droplets in place. The tygon tubing delivery system allows us to select only those portions of the throughput that we want. Unstable or off size microencapsulated droplets produced during start-up or during flow adjustments can be discarded. We are also able to select and separate subsets of microencapsulated droplets from the same run to study different gelling techniques. Because of the success of this droplet generator we have totally abandoned the "shake and toss" technique.

In order to initiate polymerization of the monomer in the organic phase, it is necessary to deliver the microencapsulated droplets into a heated environment. With shake and toss we had been dumping them into a hot, aqueous PVA solution stirred by a low shear blade, with the result of considerable breakage and some size decrease due to the shear of the rotating blade. We have now adapted a technique developed at WJSA, and deliver our microencapsulated droplets into a PVA solution in a flask heated by a water bath and attached to a rotary evaporator set-up. The rotary evaporator agitates the suspended droplets by rotating the collection vessel. Because there is no stirring blade, the droplets are not cut and maintain their original size. We have produced shells with diameters of less than a millimeter to several millimeters by using this orifice and the rotary evaporator system. Photos of sample shells are shown in Figures 2a and b. The shell shown in Figure 2a has a wall thickness of 100 µm and an OD of 1.2 mm. Figure 2b shows the uniformity of a batch of shells.

The foam shells produced by the orifice and rotary evaporator have a narrow size distribution, but often severe P1 defects. Both features can be seen in Figure 2b. In some cases the microencapsulation layer breaks, releasing the internal water droplet and forming an oil droplet that results in a foam bead. The P1 defects are not caused by the droplet generator, but are a function of the conditions during gelation. We recognize that this may be the key problem to overcome in producing usable targets. However we first need to confirm that we have a neutrally buoyant system at our gelling temperatures, and that we have adequate control of the microencapsulated droplet dimensions. We must also understand the polymerization and gelation kinetics (see below). Once we understand these aspects of the problem and have good density matching, we can begin to explore possible routes to symetrization of the wall. T. Wang has published work[9,10] focusing on this problem that will be explored. H. Kim at LLE has indicated that his group (as well as the Osaka group) will also be working on this problem.

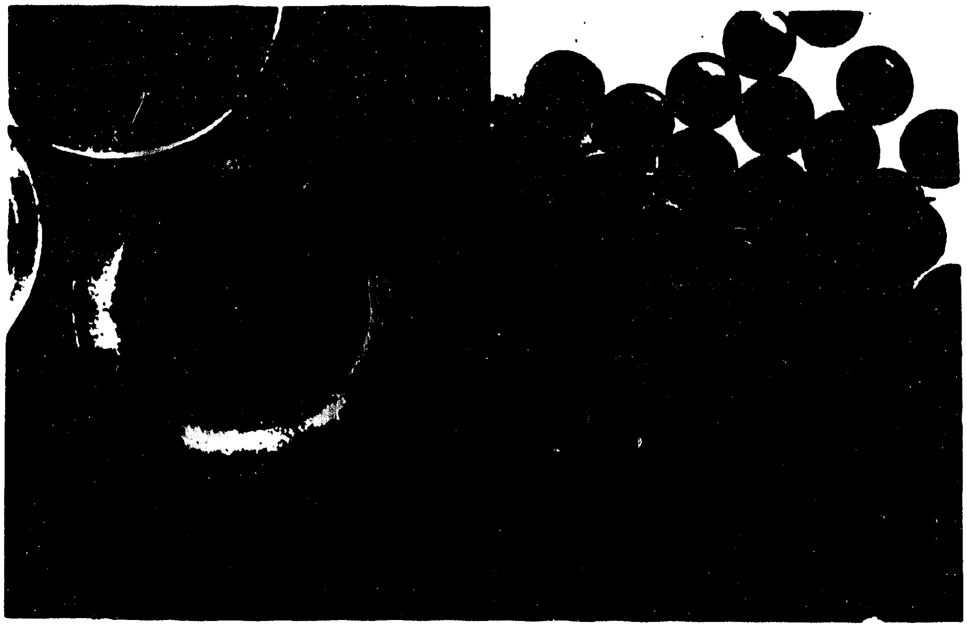

Figure 2. **a.** An individual foam shell in ethanol (darkfield microscopy). The diameter of this shell is 1.19 mm, it has a 120 µm thick wall. **b.** Sample of shells produced by the new droplet generator. Note the consistent diameter but significant P_1 defects. These shells are approximately 1.1 mm in diameter.

Polymerization and Gelation Issues

A problem that confounded us through much of this period was that the polymerization (and thus gelation) rates appeared to be slowing relative to our earlier work, resulting in structurally unstable shells in many cases. This had in fact been an occasional problem in the earlier batches but seemed to become more pronounced when we adopted some of the changes to the process reported during Norimatsu's visit.[6] Specifically, the solvent for the oil phase of the foam was changed to pure dibutyl phthalate whereas it had been a 50:50 mixture of dibutyl phthalate and diethyl phthalate. This is a welcome change since the density of the oil phase now more closely matches that of water and the shells are more neutrally buoyant. It was also reported by Norimatsu that the temperature of gelation was reduced to 80 °C (a drop from the previously reported 90 °C). This is also welcome since it is difficult to drive 1500 mL of aqueous PVA solution to 90 °C on a hot plate. Unfortunately even at 95 °C we were often unable to make an adequately crosslinked foam, and upon washing and pouring the shells into toluene they would disintegrate.

J. Rosenberg and P. Flodin have written a series of excellent papers[11-15] on the gelation of trimethylolpropane trimethacrylate (TMPTMA) using 2,2'-azobisisobutyronitrile (AIBN) in a variety of solvents. They divided the polymerization into three steps. The first is the solution polymerization before gelation and represents growing linear chains of polymer. The point of initial gelation occurs at the end of this phase, still at very low conversion (~5%) and is probably due to the physical entanglement of the linear chains. In the second phase of polymerization, chemical crosslinks are formed with one of the unreacted vinyl groups of these chains, probably at points of entanglement. Subsequent polymerization occurs from this framework until all the monomer is consumed or the pendant double bonds can no longer react for steric reasons.

We reasoned that the droplets were gelling (due to the observed shell cloudiness) but that crosslinking was not occurring. Our first thought was that there was insufficient active initiator and efforts were made to recrystalize this material. We even went to the effort to destabilize the monomer, however despite these efforts, the polymer in the shells still would not crosslink sufficiently to give stable structures. We were puzzled by this since we could make bulk foam in ampoules, but in the encapsulation process crosslinking would not occur. It was hypothesized that bulk foams formed because the polymerization was exothermic allowing for heat build up, while in the encapsulation process any excess heat would be quickly transferred to the surrounding aqueous phase. An experiment where a thermocouple was cast in a bulk sample did show an exotherm which may confirm our hypothesis.

This hypothesis, however, did not supply an answer to the incompletely crosslinked foam in the encapsulated droplets. The Osaka reports[6] called for a degassing of the oil phase prior to encapsulating the inner phase. We assumed this was to remove dissolved gasses (especially oxygen) which are known to act as chain transfer agents during radical polymerization. This is especially important when trying to create high molecular weight linear polymers, but in our situation where the polymer is to be highly crosslinked, it did not seem to be particularly important. We had been degassing by placing the oil phase in a gas-tight syringe, capping the nozzle, and pulling back the plunger to create a vacuum. The released gas bubbles were allowed to surface and then were expelled out the nozzle.

In an effort to more closely duplicate the Osaka process we placed the oil phase in a vacuum desiccator at 90 mT. Dibutyl phthalate is a high boiling solvent (BP 340 °C) and thus has a very low vapor pressure at room temperature. The solution was observed to slightly boil at about 600 mT and again at about 300 mT, but then boiled again vigorously (sometimes after some period of time) at about 90 mT.

The results of this degassing procedure on the subsequent polymerization was significant. In order to quantify the changes and compare with measurements made previously, we ran the polymerization reaction in our Couvette viscometer to measure the time to gelation. Figure 3 shows the viscosity as a function of time at 70 °C for the systems as degassed at 90 mT and as previously done in a simple syringe. Note that the time to gelation was reduced more than a factor of two.

In an effort to isolate the unknown contaminant that was removed during the degassing, the solvent was degassed in the presence of a liquid nitrogen cold finger. The collected material was melted and injected into a GC-FTIR. A single peak was eluted from the column and identified by its IR spectra as being isopropanol. Figure 4 shows the IR spectra of the unknown with the Sadtler IR library spectrum of

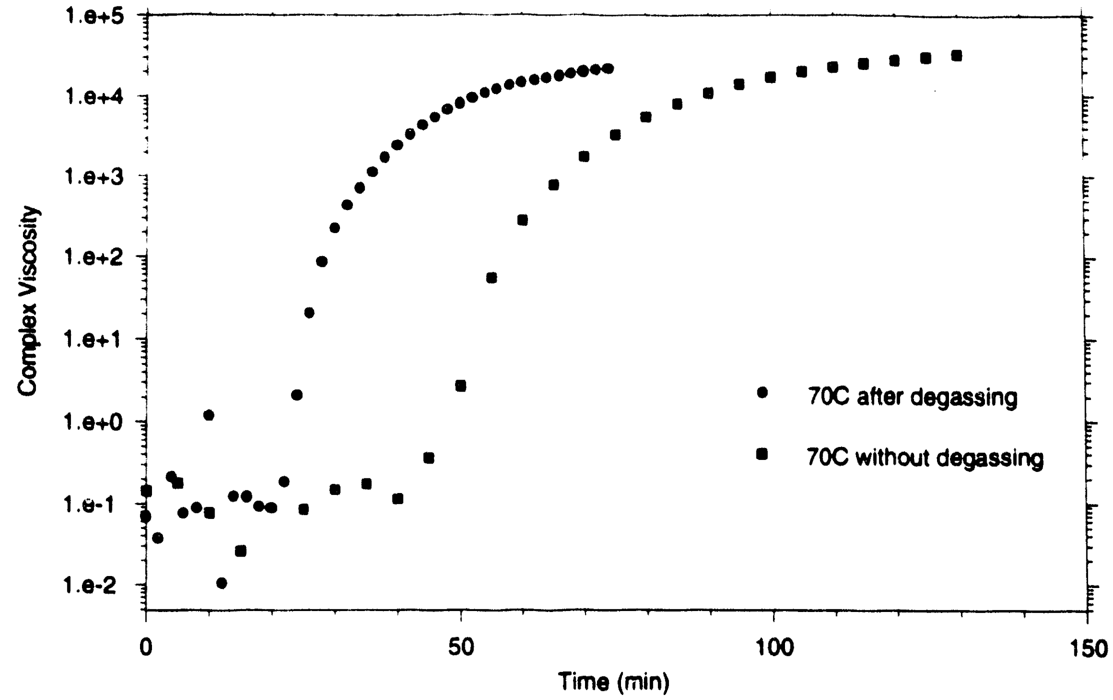

Figure 3. The viscosity of the oil phase is shown as a function of time for samples where the solvent has and has not been degassed. The sharp rise marks the onset of gelation.

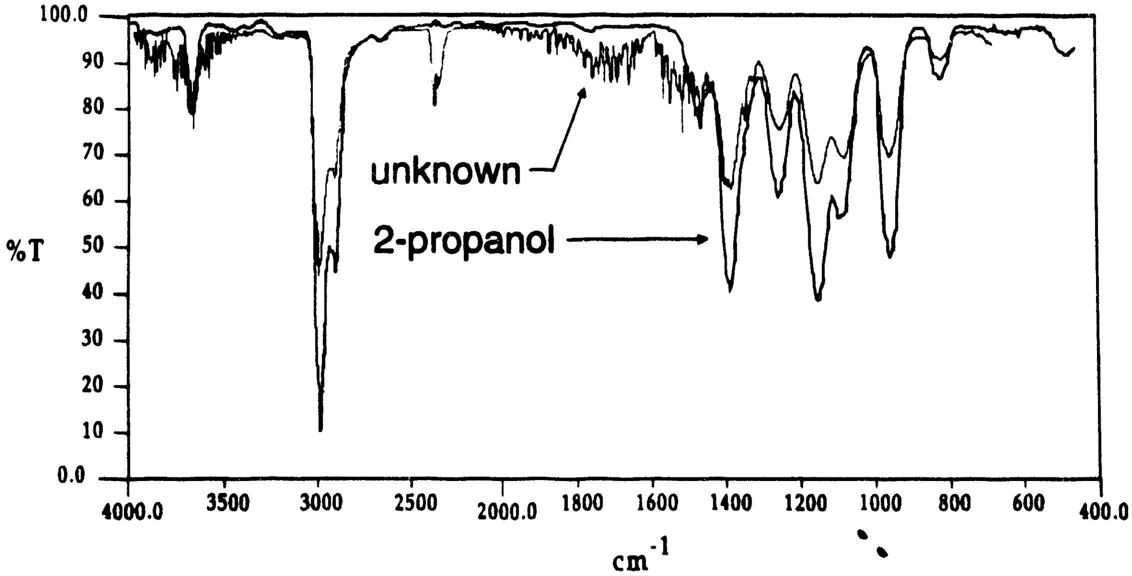

Figure 4. Shown is the IR spectra of the unknown extracted from the dibutyl phthalate with the Sadtler IR library spectrum of isopropanol overlaid for comparison. The agreement provides strong evidence of isopropanol contamination of the dibutyl phthalate.

isopropanol overlaid for comparison. The presence of significant quantities of isopropanol in the solvent would have the effect of consuming initiator, and thus may explain the reduced polymerization rate and lack of crosslinking. It is not clear, however, why isopropanol should be present as a significant contaminant in dibutyl phthalate. A literature search did turn up a reference to a synthetic process for making dibutyl phthalate that involved a trans esterification using Bu_2SnO and $(i\text{-PrO})_4Ti$.[16] It is possible that isopropanol is used as a solvent for the process and was not completely removed. As a simple test of the effects of small amounts of isopropanol on the polymerization, a drop of isopropanol was put in four ampoules of the oil phase each containing the polymerizable monomer and initiator. The ampoules were then placed into an oven at 80 °C. After several days, none of the solutions polymerized.

As an additional check on our suspicions, we had the solvent purity analyzed by GC-MS in Chemistry. They found no isopropanol, though they did find small amounts of other contaminants. Thus the situation remains unresolved. We continue to have difficulty in the polymerization and gelation/crosslinking stages. While we have experienced an increase in the rate of polymerization by rigorously degassing the oil phase, we are still experiencing a frequent loss of the internal phase during polymerization with the result that most of our product is foam beads. The inner phase appears to simply break out through the top of the oil shell at around ten minutes at 90 °C. Unfortunately we don't see the oil phase go through cloud point until around 15 to 20 minutes. Clearly getting these problems resolved is of the highest priority.

Solvent Exchanges and Increasing Process Efficiency

Once the microencapsulated droplets are formed, and polymerized to form the dibutyl phthalate filled foam shell, there follows a series of time consuming solvent exchanges as noted in the process summary in the Introduction. These exchanges are nothing more than repeated simple dilutions of the solvent in the foam capsule with a new solvent. If equilibrium is reached and 90% of the mixed solvent is discarded each time, then three exchanges will remove all but 0.1 % of the original solvent. A key question, if exchanges are to be done manually, is how long does it take to equilibrate the new solvent with the solvent in the shells. While preparing bulk foams for light scattering measurements (see below) we measured the time to equilibrium for the exchange of toluene by ethanol by measuring toluene content in the ethanol-toluene soaked shell mixture as a function of time by gas chromatography (GC). Figure 5 shows that equilibrium is reached in around four hours. For greatest throughput efficiency one should certainly exchange the solvent before that.

However, the best situation would be if the solvent could be continuously exchanged. To that end, we have constructed a Soxhlet extractor for the initial exchange of toluene for dibutyl phthalate. A schematic of the set up is shown in Figure 6.

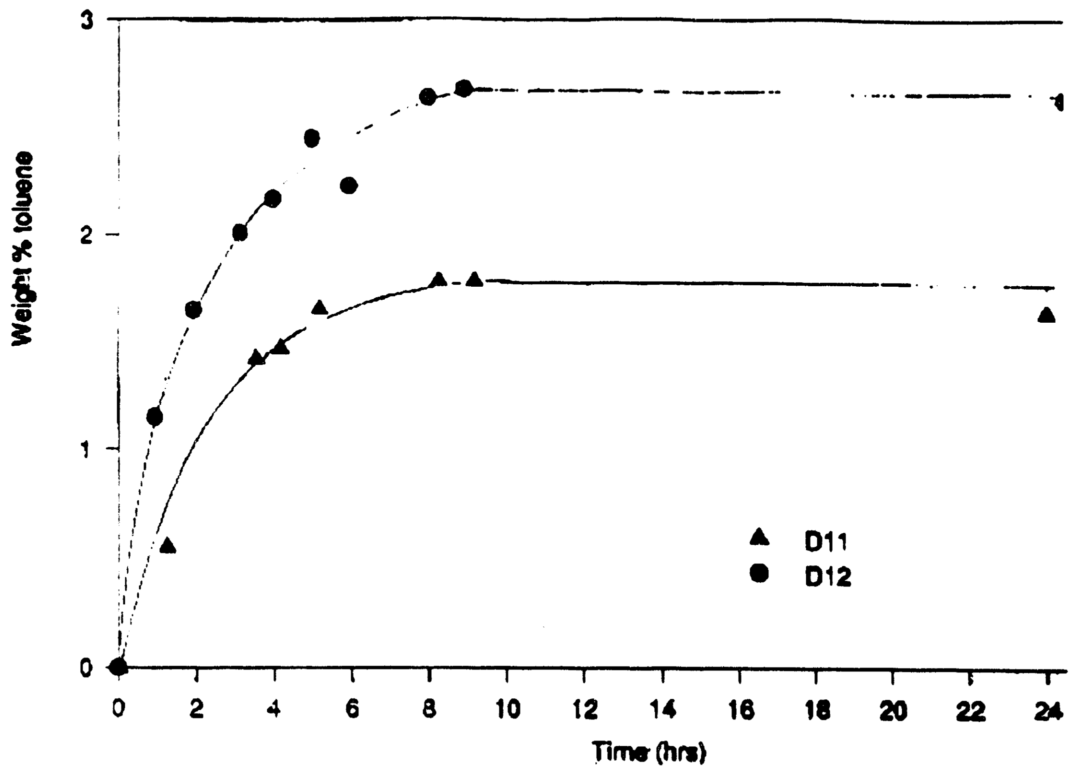

Figure 5. Plots of toluene concentration in an ethanol bath as a function of time for two different bulk foam samples show that equilibrium is reached in about 10 h. Concentration was measured by GC.

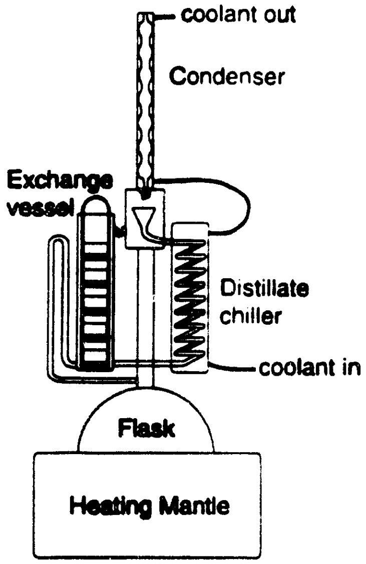

Figure 6. A schematic of a Soxhlet extractor that has been constructed for the initial exchange of toluene for dibutyl phthalate is shown.

This system fills and dumps automatically on about a fifteen minute cycle. The shells are loaded into crystallization dishes which are in turn loaded into a rack which fits in the exchange chamber. The toluene remaining in the recrystallization dish during each dump prevents the shells from drying out. As the exchange chamber is external to the Soxhlet and the distillate is cooled prior to entering the chamber, the rack can be removed at any time without interrupting the distillation process. Dibutyl phthalate does not azeotrope with toluene and has an extremely high boiling temperature (340 °C) so the purity of the extracting toluene is quite high. As a significant side benefit we have virtually eliminated our toluene waste stream.

A similar system is being built for the next exchange of ethanol for toluene, with a few modifications due to the fact that toluene (BP 110.6 °C) and ethanol (BP 78.3 °C) form a minimum boiling azeotrope (68% ethanol and 32% toluene, BP 76.7 °C). This

Soxhlet will have the ability to distill off the azeotrope from time to time to clean up the toluene contaminated ethanol in the reservoir. Since the amount of toluene in the system is small relative to the amount of ethanol that will collect in the exchange dishes, it may not be necessary to azeotrope off the toluene during the exchange, especially since the next exchange will introduce *p*-chlorotoluene. What is important is that all the traces of water (left after the first exchange of toluene for dibutyl phthalate) are removed by the ethanol. Thus a single clean-up of the exchange solution near the end of a run may be necessary to remove the low boiling water-benzene-ethanol azeotropes.

The exchange of the *p*-chlorotoluene for ethanol could also be done by these methods, however there are two problems. First the ethanol being removed will certainly form a low boiling azeotrope with the *p*-chlorotoluene that will compositionally be mostly ethanol. This azeotrope will need to be removed by distillation to insure removal of the ethanol from the system, which might otherwise react with the diacid during the overcoating process. The more difficult problem in automation is the introduction of the diacid. Almost certainly this will have to be done by manual exchange techniques.

Perhaps the most important solvent exchanges are the ones that occur after the overcoating is applied The excess acid chloride and *p*-chlorotoluene are washed out and replaced with *p*-dioxane. This can certainly be done by our Soxhlet methods since the boiling point of *p*-dioxane (101 °C) is much lower than that of *p*-chlorotoluene. Finally, the dioxane filled shells are placed in the Polaron pressure vessel and the dioxane is exchanged out with high pressure liquid CO_2. It is especially important to remove all of the dioxane from the shells before attempting to bleed off the supercritical CO_2, since any remaining dioxane will crush the foam due to capillary forces. Because it is both frustrating and expensive to lose shells in the last step of the process, we are designing a system to analyze the liquid CO_2 solvent composition in the Polaron to insure complete exchange prior to taking the system supercritical and bleeding off the CO_2.

GC standards to evaluate the efficiencies of the exchanges and the composition of the exchange fluids have been prepared for toluene, ethanol, *p*-chlorotoluene, and dioxane, and from them the FID response factors have been determined. Quantitative analysis of any of the solvent combinations (excepting water) that normally arise within the exchange processes can thus be made rapidly.

Shell Overcoating

Because of the problems with polymerization and gelation discussed above, not many batches were overcoated. We began by overcoating with the hydroxyethyl cellulose (HEC) system, but have recently done trial batches with the poly(vinyl phenol) (PVP) system. Our focus here was largely historical. The HEC system has been extensively reported upon and experimentally has some nice features, specifically that the coating grows linearly with time (suggesting that the rate limiting step is the diffusion of the HEC to the surface), and that pH control with a Na_2CO_3 buffer system is convenient. However in recent conversations with Norimatsu and with Hyo-gun Kim, the prevailing opinion has been that the PVP overcoats produce smoother surfaces. Thus, we intend to focus now on PVP coatings.

Our limited work with the HEC system has been instructive. We have made an interesting use of this polycondensation technique to produce large (1 -3 μm) thin walled, full density (no foam layer) microshells, an idea that originated with H. Kim at LLE. These shells were formed by running the diacid solution through the droplet generator without an inner water phase and stripping the formed droplets with HEC solution. We had previously noted that the polycondensation reaction would occur on the outside of a diacid droplet in the absence of a foam layer, and a shell made only from diacid crosslinked HEC would form. It is for this reason that the diacid filled shells are rinsed repeatedly in PVA solution to remove all the excess diacid prior to introduction to the HEC solution in the foam shell overcoating process.

In making these simple HEC shells, we discovered a process problem that also impacted overcoated foam shells. We had noted that the outside surfaces of some batches of our HEC overcoated foam shells and simple HEC shells were characterized by a blistered appearance. Figure 7 shows a cracked simple HEC shell in which the surface is covered with these small blisters and craters. Close evaluation of the wall profile along the crack edge shows nothing to suggest that the blistering occurred over the entire formation process but was rather unique to the outer surface. This suggests that the bubbles must have occurred during the neutralization steps that are taken to terminate the HEC - diacid interfacial reaction. There are several possible explanations, however a leading candidate is that the neutralization of the Na_2CO_3 buffer with HCl, which is done to terminate the HEC - diacid reaction, resulted in the generation of CO_2 bubbles. This might occur if the solution is taken too acid. We were using concentrated HCl for this step, but we found that when a more dilute HCl solution was added over a longer period of time, the blistered surface disappeared. Figure 8 is an SEM of a dried, overcoated, foam shell produced after this correction was made. This surface is comparable to what we obtained in earlier batches but is admittedly still unsatisfactory.

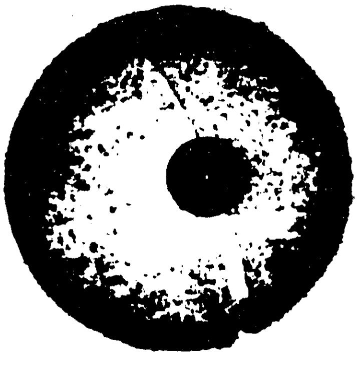

Figure 7. Shown is a cracked, HEC shell without foam liner in which the surface is covered by small blisters and craters. Dark spot at the pole position is a trapped air bubble. (50X magnification)

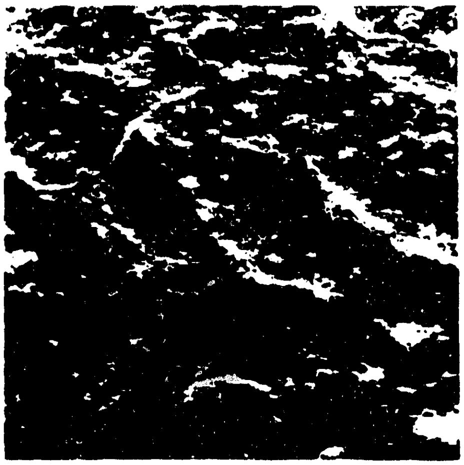

Figure 8. Shown is an HEC overcoated foam shell produced after we had reduced HCl concentration and slowed its addition. All evidence of the blistering is gone. (1000X magnification)

We have chosen to postpone further work with the HEC. It may require significant effort to improve its surface finish and reports from Osaka[4] indicate that the PVP system can produce a 0.2 micron surface finish. This is ultimately not good enough, and will need improving to about 0.05µm. We have just begun using the process, but it does appear that the PVP surfaces tend to be smoother. However, there is another process problem. It is more difficult to obtain a tight fit of the PVP coating to the foam. We will try to correct this by using various washing techniques to remove excess diacid solution from the shell exterior before exposing them to the PVP solution. It will also be useful to make simple PVP shells, as we did with HEC, to study surface finish.

Foam Light Scattering Experiments

One of the concerns raised by the Cryogenic Group is that the foam in these shells scatters light too much to allow visual measurements of the thin D_2 liquid-layered overfill. This is because the void size within the foam is on the same length scale as the wavelength of the probe light. We are working with Jorge Sanchez to create samples and make measurements to quantify the problem. It will be several months before Sanchez has a cryostat in which he can make low temperature measurements on samples. In the meantime, we are trying to make room temperature measurements of transmission and scattering as a function of wavelength on foam samples.

The IR spectra of a foam shell is displayed in Figure 9. The absorption bands in this spectrum are due to the vibrational modes of the polymer molecules. A transmission window is present between 3600 and 5500 nm.

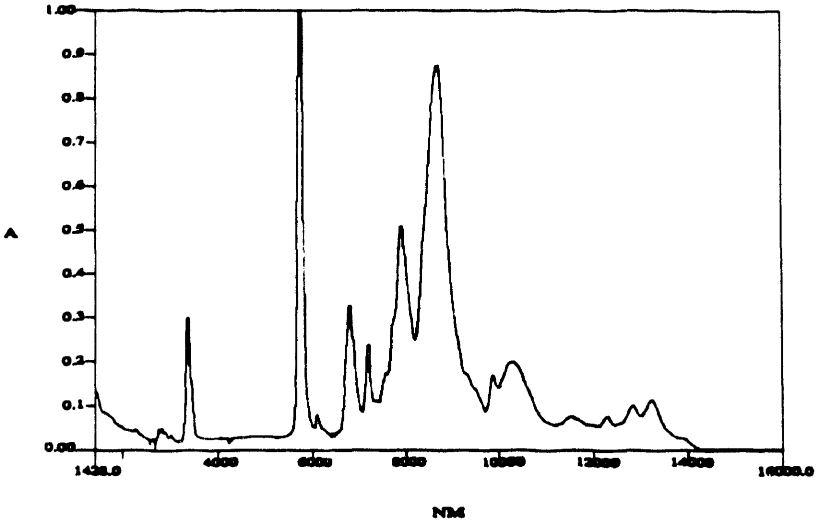

Figure 9. The IR absorption spectra of a foam shell is shown. The absorption bands in this spectrum are due to the vibrational modes of the polymer molecules. A transmission window is present between 3600 and 5500 nm.

Figure 10 shows the spectrum into the near IR. This was taken by placing an IR 5X beam condenser in the sample path of our Perkin Elmer Lambda 9. The large anomaly between 800 to 900 nm is due to a grating/source change in the instrument. Since the optics for the beam condenser were designed to operate in the IR region, the data at visible wavelengths is subject to question. However the near-IR region appears to be interference free. The increasing absorbance as you move towards the visible region is probably due to increased scattering within the sample.

In order to perform quantitative measurements on the degree of scattering, we needed to create thin (~500 µm) foam windows. Bulk samples of gel have been processed into large foam cylindrical samples (2 cm diameter x 4 cm long) which have been cut into windows using TS&T's excimer laser. Figures 11a and b show the surface of foam material cut in this manner. On the microscopic level, the damage seen in Figure 11a should have no effect on the degree of scattering. On the macroscopic level, the striations seen in Figure 11b are significant and result from the roughness of the mask used. Efforts are underway to try to eliminate them by moving the mask while cutting.

To experimentally quantify the degree of optical access that will be available in the future cryogenic layering experiments, the foam samples which have a refractive index *n* of 1.55 will be filled at room temperature with fluids that will mimic the effects of liquid deuterium (*n*=1.13). There are two options. If available, we can use a liquid that matches the *n* of liquid deuterium, or we can use a liquid that has the same foam-deuterium mismatch, but the difference is caused by a higher index liquid.

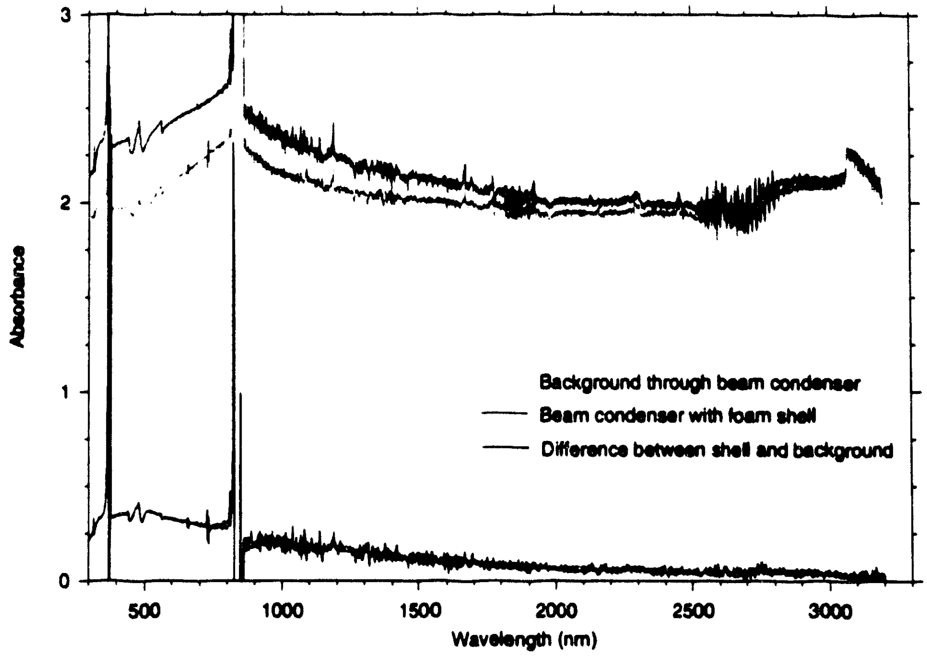

Figure 10. The visible and near IR absorbtion spectra of a foam shell is shown. The large anomaly between 800 to 900 nm is due to a grating/source change in the instrument.

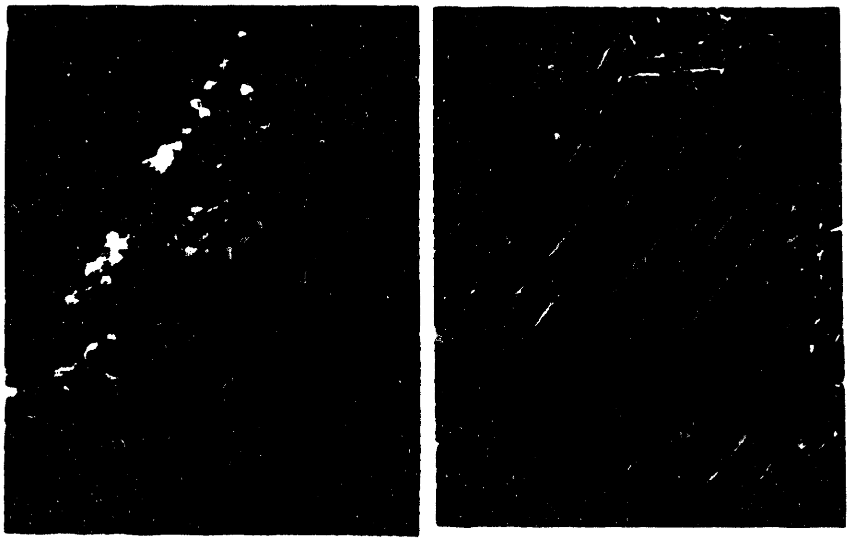

Figure 11. The surface of low density foam cut with an excimer laser is shown. **a.** On the microscopic level some damage is seen in the form of local densification, probably from local melting. **b.** On the macroscopic level, significant striations are seen which result from the roughness of the mask used.

Cargille is the standard source of index matching fluids, but they do not supply them below 1.3 or above 2.11. A literature search found some possible candidates for the low index. The first, ethylidene diacetate, has a published value of 1.070 at the sodium line. Since virtually all simple organic compounds have indexes in the 1.35-1.6 range, this reported value may be a typo (it is also listed as 1.070 in the CRC, but they may have simply repeated the typo). The supplier was also contacted, but they could not confirm the number. We ordered some, and after receipt we will confirm the index with a refractometer. Its other properties and lack of toxicity make it quite attractive for our purposes. If the ethylidene diacetate proves to be unsuitable, a member of the perfluoro alkanes, which have more believable indices of from 1.251 to 1.262 can be tried.

To match the H_2-foam index mismatch on the high side we would need a fluid with index of about 2.1 (effect of mismatch goes as $(n_1-n_2)^2/(n_1+n_2)^2$). Known fluids with high indices (available from Cargille) tend to be very viscous, dense, dark in color, and often reactive. We are concerned that they will not wet the foam, or may crush it through capillary action, or may possibly react with the foam. If neither the identified low index chemicals nor the available Cargille high index liquids are appropriate, we will look further in the literature for other possible high index chemicals.

Current Plans

We have made progress in duplicating the ILE process. The significant achievements are the building of a droplet generator and the improvements to process efficiency. Good progress has been made in understanding the spectral qualities of the foam. Three problems remain: loss of the inner phase during polymerization, bad P1 defects, and poor surface finish on the polycondensation polymer overcoat.

We will seek solutions to the loss of the inner phase in a number ways. First, we will look for ways to increase the rate of polymerization and crosslinking in the oil phase. This will include a careful purification of the oil phase solvent by fractional distillation. In addition we will test the effect of additional initiator on the rate of gelation. We can also test the effect of increased monomer concentration. While this last solution has the negative effect of increasing the foam density, it should increase the rate of polymerization and may also increase the viscosity. In the short term the higher density would be acceptable to produce targets for LLNL cryogenic studies and may have the added advantage that a smaller cell size could aid optical transparency. All of these tests of gelation rate can be rapidly tested on the Rheometrics. Second, we will improve the density matching of the inner water phase with the oil phase. Currently, the inner water phase is less dense than the oil phase at all temperatures (up to 100 °C). We will lower the oil phase density slightly by blending in less dense toluene. Third, we will explore ways to increase the viscosity of the oil phase with the expectation that a more viscous oil phase will retard the motion of the inner aqueous phase. This last approach is complicated, and will be delayed pending the results of other approaches.

Our exploration of P1 defects will be delayed until we solve the stability of the inner phase problem, since the two are clearly coupled. As noted earlier, this is perhaps ultimately the most difficult problem to solve. Also as noted earlier, we have already begun to turn our attention to overcoating with PVP to improve the surface finish of the overcoated shells. We will be talking further with Hyo-gun Kim about the details of the process, and will also discuss the process extensively with Takagi during his visit this spring.

References

1. Chen, C.; Norimatsu, T.; Takagi, M.; Katayama, H.; Yamanaka, T.; Nakai, S. *J. Vac. Sci.* A **9**, 340 (1991).

2. Takagi, M.; Norimatsu, T.; Yamanaka, T.; Nakai, S. *J. Vac. Sci.* A **9**, 820 (1991).
Takagi, M.; Ishihara, Nakajima, K.; Norimatsu, T.; Izawa, Y.; Yamanaka, T.; Nakai, S. *Kaku Yugo Kenkyu (Nuclear Fusion Research)* **68**, 281 (1992).

3. Takagi, M.; Ishihara, Nakajima, K.; Norimatsu, T.; Yamanaka, T.; Nakai, S. *Kobunshi Ronbunshu (Polymer Thesis)* **49**, 661 (1992).

4. Takagi, M.; Ishihara, M.; Norimatsu, T.; Yamanaka, T.; Izawa, Y.; Nakai, S. *J. Vac. Sci.* A **11**, 2837 (1993)

5. Takagi, M.; Ishihara, Nakajima, K.; Norimatsu, T.; Yamanaka, T.; Nakai, S. "Fabrication and characterization of overcoated low density foam shell for inertial confinement fusion" presented at AVS. 39th Nat. Sym., Nov. 9-13, 1992, Chicago.

6. Norimatsu, T.; Chen, C. M.; Nakajima, K.; Takagi, M.; Izawa, Y.; Yamanaka, T.; Nakai, S., "Cryogenic targets and related technologies at ILE Osaka University" presented at AVS 40th National Symposium, Nov. 15-19, 1993, Orlando, Florida.

7. Hyo-gun Kim, "Plastic-Layer-Overcoated, Low-Density Foam Shells Are Fabricated Using the Microencapsulation Technique Followed by Interfacial Condensation Polymerization" presented at The 9th Target Fabrication Specialists Meeting, July 5-9, 1993, Monterey, CA

8. Hyo-gun Kim, "Fabrication of Foam Shells Overcoated With Plastic Layers", *LLE Review* **56**, 216 (1993).

9. C. Lee and T. Wang, *J. Fluid Mech.* **188**, 411 (1988).

10. T. Wang, "Dynamics of Thin Liquid Sheets" presented at AIP Third International Colloquium of Drops and Bubbles, 1988, Monterey, CA, (AIP Conference Proceedings 197).

11. P. Flodin andP. J. Lagerkvist, *Chromatogr.* **215**, 7 (1981)

12. J.-E. Rosenberg and P. Flodin, *Macromolecules* **19**, 1543 (1986).

13. J.-E. Rosenberg and P. Flodin, *Macromolecules* **20**, 1518 (1987).

14. J.-E. Rosenberg and P. Flodin, *Macromolecules* **20**, 1522 (1987).

15. J.-E. Rosenberg and P. Flodin, *Macromolecules* **21**, 2041 (1988).

16. R. H. Stanley, D. W. Brook, and V. Prenna, (British Titan Products Co. Ltd.), "Synthesis of esters by transesterification.", German Patent DE 1807103 691218, Chem. Abst. 72(9):42829u.

DATE FILMED

6/23/94

END